Proceedings of the 30th International Cosmic Ray Conference
Rogelio Caballero, Juan Carlos D'Olivo, Gustavo Medina-Tanco,
Lukas Nellen, Federico A. Sánchez, José F. Valdés-Galicia (eds.)
Universidad Nacional Autónoma de México,
Mexico City, Mexico, 2008

Vol. 5 (HE part 2), pages 1175–1178

30TH INTERNATIONAL COSMIC RAY CONFERENCE

Electromagnetic and muon primary discrimination from underground scintillator signatures

F. SANCHEZ[1], G. A. MEDINA-TANCO[1], E. NAHMAD-ACHAR[1], J. C. D'OLIVO[1], J. F. VALDES GALICIA[2].
[1] *Instituto de Ciencias Nucleares , Universidad Nacional Autónoma de México, México, D.F., C.P. 04510,*
[2] *Instituto de Geofísica, Universidad Nacional Autónoma de México, México, D.F., C.P. 04510,*

federico.sanchez@nucleares.unam.mx

Abstract: We describe the end-to-end simulation of the muon telescope detailed in [1]. The simulations include (a) the shower evolution in the atmosphere, (b) the propagation of secondary cascades through the ground, (c) the photon emission inside the scintillators, (d) their propagation in the plastic and eventual absorption by the wavelength shifter inside the optical fibers and (e) emission and propagation inside the fiber and up to the window of the PMT. Spatial information coming from the simulations is then used to analyze the efficiency of neural networks for the statistical discrimination of particle tracks derived from high energy electrons/photons and muons impinging the ground.

Introduction

Extensive air shower (EAS) simulation codes are widely used by the high energy cosmic ray community. Although there are many uncertainties related with the hadronic interaction models used to simulate the first interactions in the cascade, most codes are known to reproduce quite well the central regions of the particle distribution functions. At higher energies, the scenario is complicated because of the impossibility of simulating the huge amount of secondary particles that are produced in a real shower. In order to circumvent this problem, different thinning algorithms are built into the codes, adding further uncertainties to the simulation results. Nevertheless, any ground based experiments must rely on simulations to interpret their measurements. In an accompanying paper [1], we describe an experiment we are building at the ICN-UNAM falicities in order to measure the electromagnetic to muon ratio at ground level for showers beyond 6 PeV. This buried muon telescope might shed light on some of the above mentioned uncertainties and, at the same time, contribute to the physics involved in EAS development. In this work we present the end-to-end simulations of the above mentioned experiment, as well as a neural network analysis approach that might be used to disentangle the muonic and electromagnetic signatures in the detector.

End-to-end simulations

The machinery we implemented in order to have realistic end-to-end simulations for our experimental setup [1] starts with the interaction of the primary cosmic ray with the atmosphere, follows with the shower development in air and its propagation underground, and finally ends with the detector simulation. The former steps are performed with the Aires package [2] while the propagation underground, as well as the detector response, are simulated with the Geant4 package [3] as schematically shown in Figure 1. The shower cores were uniformly distributed within a triangular array of 3 water Auger-like Cerenkov detectors separated 200 m from each other. A three-fold coincidence signal of 3 vertical equivalent muons (1 VEM $\sim$ 250 MeV of energy deposition) in the tanks is used as trigger condition. The secondary shower particles that fall over the area above the scintillator planes and cross the volume enclosed by

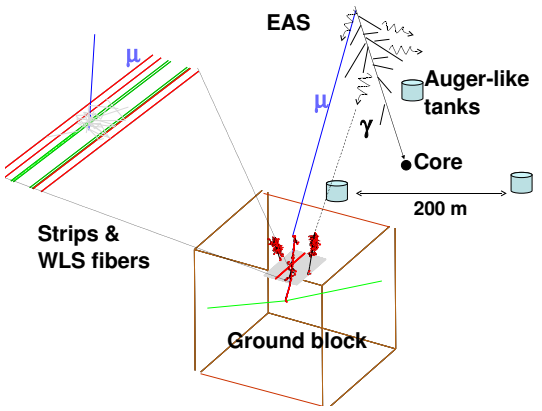

Figure 1: Schematic view of the end-to-end machinery simulation (for the sake of simplicity, only one scintillator plane is shown).

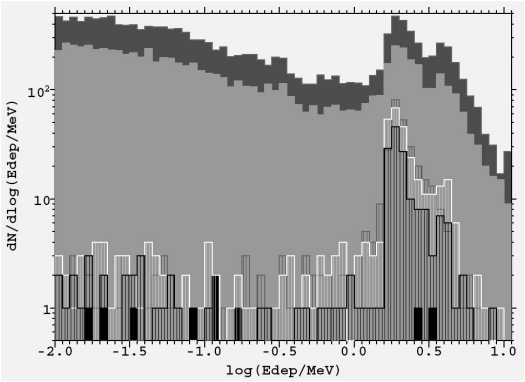

Figure 2: Energy deposition per plane. Solid histograms are the energy deposited in the first two scintillator planes by γs and $e^{\pm}$s while open histograms correspond to muons. The plane depths are 0.25 m, 0.50 m and 2.50 m for the first, second and third respectively.

the detector are then propagated underground until they reach the scintillator strips. The soil density was set to 1.8 g/cm^3 with a mean charge and atomic mass of $\langle$Z$\rangle$=11 and $\langle$A$\rangle$=22 g/mole respectively. As a first approach, the scintillator strips were assumed to trigger for an energy deposition $\geqq$ 300 keV without taking into account the attenuation length of the WLS fibers (see [1] for further datails).

The underlying idea beneath any discrimination algorithm lies on the different characteristics of the underground propagation between muons, gammas, electrons and positrons. While muons propagate ballistically with little angular deviation, electrons and photons develop underground subshowers. Although most of the energy of these sub-showers is concentrated within the Moliere radius (which is $\sim$ 5 cm in our case), it is expected that the signatures left by impinging γ or $e^{\pm}$ are broader than the corresponding muonic signatures. However, the exact features will depend on the initial energy of the parents hitting the ground and the depth and space resolution of the detector.

The differences in propagation mentioned above can be appreciated in Figure 3. Since the mean energy of muons at ground, for cosmic primaries of PeV energies is a few GeV, they are expected to cross the three scintillator planes triggering one strip per layer. Therefore, their signature will be an xy-cross of triggered strips per plane and, above $\sim$ 1 GeV, they are expected to cross the three planes. On the other hand, γ and $e^{\pm}$ are much less penetrating and are likely to trigger more than one adjacent strips per layer.

Figure 2 shows the energy deposited by the muonic and the electromagnetic components in each detector plane for a $10^{15.6}$ eV induced proton shower. It can be seen that the γ and $e^{\pm}$ are more abundant, but deposit energy mainly in the first and second planes. The shape of the energy deposit distribution from 10 keV to 1 MeV is related to the shape of the energy spectrum at ground and is produced by particles that stop at the detector. The peaks at $\sim$ 2 MeV are produced by the cores of the subshowers which cross completely the strips. Muons, on the other hand, deposit almost the same amount of energy in the three planes.

Event discrimination by artificial neural networks

The simulations described above have been used to generate γ, $e^{\pm}$, and $\mu^{\pm}$ events with the space and timing characteristics expected from the detector. These events, covering the energy range of interest, from 100 keV to 3 GeV at 0.1 MeV steps with a flat spectrum, are used for discrimination studies between muons ($\mu^{\pm}$) and electromagnetic com-

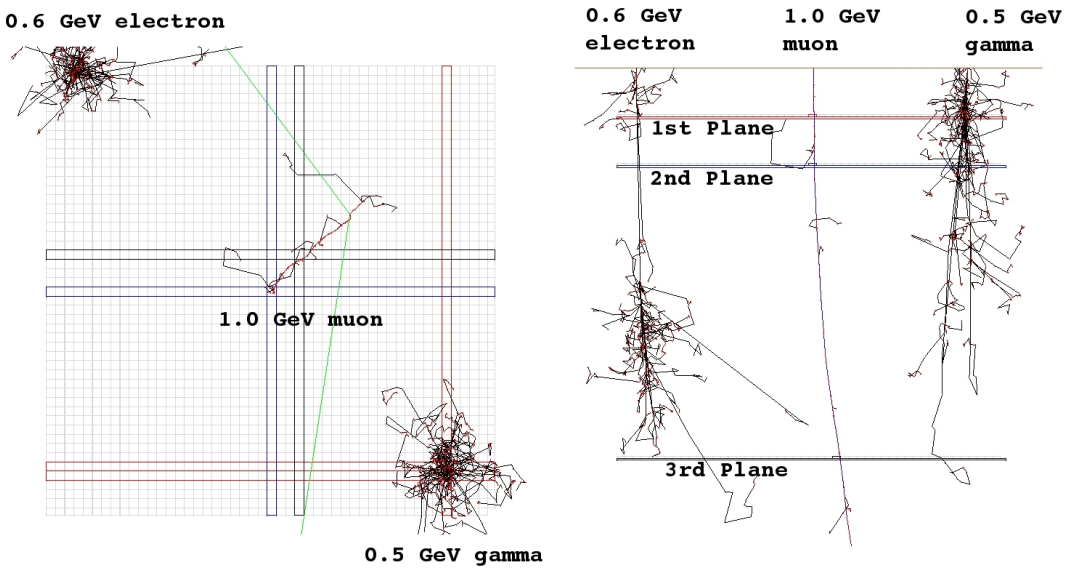

Figure 3: Top and side views of one simulated event with 3 different impinging particles. Triggered strips are colored (red=1st plane, blue=2nd plane, black=3rd plane). The plane depths are 0.25 m, 0.50 m and 2.50 m respectively.

ponents (gammas (γ) and electrons ($e^{\pm}$)). To this end, we constructed an Artificial Neural Network (ANN) capable of associating measurements with known classes or groups, and capable of adjusting itself ("learning") according to situations presented to it. ANN's use a complete set of functions which form a basis of $C^0[0,1]$, the vector space of continuous functions in $[0,1]$, and can thus approximate any behavior of the data without any guesswork. The ANN used are feed-forward backpropagating networks.

As described above, the detector consists of 3 planes (hereafter named $P_1,\ P_2,\ P_3$) at different depths, each having 2 layers (labeled x and y, with x always lying below y). Each layer is made of 50 detection bars $x_i, y_i = 1, ..., 50$ which by themselves define our coordinate system: bars in layer y lie perpendicular to those in layer x.

Since sub-showers often trigger more than one bar at a given layer, we take the centroids $< x >$ and $< y >$ of the produced footprint as the coordinates for the shower on the corresponding plane; from translational invariance on the planes, the variables that have physical importance will be the *coordinate differences* between planes:

$$\Delta_1 x = < x >|_{P_2} - < x >|_{P_1}\,,$$
$$\Delta_2 x = < x >|_{P_3} - < x >|_{P_2}\,, \qquad (1)$$

and similarly for y. For both x and y, we make the following conventions for events that do not reach one or more of the planes: i) if only P_1 is triggered, $\Delta_1 = \Delta_2 = \infty$; ii) if only P_2 is triggered, $\Delta_1 = -\infty,\ \Delta_2 = \infty$; iii) if P_1 and P_2 are triggered, but not P_3, then Δ_1 is finite and $\Delta_2 = \infty$; iv) if only P_2 and P_3 are triggered, $\Delta_1 = -\infty$ and Δ_2 is finite.

Other important variables obtained directly from the detector are the number of triggered bars in each layer, $b_{ix},\ b_{iy},\ i = 1, 2, 3$. In order to give a greater weight to events in which the triggered bars are adjacent, we define

$$r_{ix} = \frac{b_{ix}}{x_{max} - x_{min} + 1},\ \ i = 1, 2, 3, \qquad (2)$$

and similarly for y. Note that $r = 1$ only for adjacent bars, and $r < 1$ otherwise. The *time differences* of triggering between planes, with con-

ventions similar to those of $\Delta_i x,\ \Delta_i y$ above, also constitute important variables that can be measured directly by the detector. We have found that this information is somewhat redundant, and chose not to use it.

$\Delta_i x,\ \Delta_i y,\ b_{ix},\ b_{iy},\ r_{ix},\ r_{iy}$ form the 16 input variables for the ANN. The output variables are $Y = (Y_1, Y_2)$, where Y_1 describes electromagnetic (γ or $e^{\pm}$) events, and Y_2 describes μ events. All input variables are normalized in $[-1, 1]$, while output variables are normalized in $[-0.9, 0.9]$. As transfer functions for the ANN, hyperbolic tangents (or "sigmoidal") functions

$$tansig(x) = \frac{2}{1 + \exp^{-2x}} - 1 = \tanh(2x) \quad (3)$$

were used for all layers except the last (output) layer, for which a linear function was chosen. For training, the scaled conjugate gradient method was used.

The ANN was trained by simulating events for all 3 types of particles with a uniform distribution in energy E, within the interval $[0.1, 3.0]$ GeV, according to the simulation model described earlier. For muons (μ) we should strictly have $Y_2 = 0.9$ (recall that $Y_2 \in [-0.9, 0.9]$). We used a tolerance $\varepsilon = 0.5$. For various network architectures, ranging from very simple to very complex, training had an overall discrimination efficiency of $\eta = 0.876$. It was observed that events with $E \leq 1.0$ GeV were very difficult or impossible to discriminate, suggesting that it is the nature of the data which prevents obtaining a greater efficiency. This cut-off energy of 1 GeV is in agreement with the expected real energy distribution of electromagnetic and muon events, as noted earlier. The simplest network built was a $2 - 1 - 2$—ANN (i.e., 2 neurons in the input layer, 1 neuron in the intermediate "hidden" layer, and 2 neurons in the output layer).

$40,000$ new data were simulated, unknown to the ANN, and following an energy distribution according with the expected real spectrum. The predictive power of the $2 - 1 - 2$—ANN was tested against this data, obtaining an overall efficiency for discrimination

$$\eta = 0.883; \quad (4)$$

with the same efficiency essentially obtained for various architectures. Restricted to muons, however, this efficiency drops to $\eta_\mu = 0.606$.

We expect only muons to reach the third plane, so that including P_3-triggers in our discrimination should increase efficiency. Indeed, in the new data we have: μevents = $8,872$; P_3-triggers = 5,366; real(μ)-P_3 coincidences = 5,366; simulated(μ)-real(μ)-P_3 coincidences = 5,327. I.e., 40% of μ-events do not reach P_3 and would be lost if accounting only for those that do; a minor number ($5,366 - 5,340 = 26$) of electromagnetic events do reach P_3; and the efficiency for discriminating as a muon an event reaching the thrid plane is

$$\eta_\mu = 5327/5366 = 0.993 \quad (\text{for } P_3\text{\_events}). \quad (5)$$

Summarizing, we can build an artificial neural network which can discriminate very well for isolated showers, with 88% prediction power overall if all events are to be accounted for; this prediction power can be raised to 99% if about half of all μ-events may be disregarded.

Conclusions

We presented a full end-to-end simulation machinery to reproduce the signatures left by the muonic and the electromagnetic components of EAS in buried scintillators. Using these simulations, we studied the discrimination potential of neural networks and demonstrated that an acceptable efficiency can be achieved in separating $\mu^{\pm}$ from $e^{\pm}$ and γ with the proposed detector presented in an accompanying paper in this conference [1].

References

[1] F. Sanchez et al., in: 30th ICRC, Merida, Mexico, 2007.

[2] S. J. Sciutto, astro-ph/9911331 AIRES: A System for air shower simulations. User's guide and reference manual. Version 2.2.0. (1999) 1–216.

[3] S. Agostinelli et al., NIM in Phys. Res. Sec. 506 (2003) 250.